frontiers | Frontiers in Cardiovascular Medicine

TYPE Original Research
PUBLISHED 06 September 2022
DOI 10.3389/fcvm.2022.960403



OPEN ACCESS

EDITED BY
Aleksandra Radjenovic,
University of Glasgow, United Kingdom

REVIEWED BY
Ruud B. van Heeswijk,
Center Hospitalier Universitaire Vaudois (CHUV), Switzerland
Tamer Basha,
Cairo University, Egypt

*CORRESPONDENCE
Markus Henningsson
markus.henningsson@liu.se

†These authors have contributed equally to this work

SPECIALTY SECTION
This article was submitted to Cardiovascular Imaging, a section of the journal Frontiers in Cardiovascular Medicine

RECEIVED 02 June 2022
ACCEPTED 05 August 2022
PUBLISHED 06 September 2022

CITATION
Jarkman C, Carlhäll C-J and Henningsson M (2022) Clinical evaluation of the Multimapping technique for simultaneous myocardial $T_1$ and $T_2$ mapping. *Front. Cardiovasc. Med.* 9:960403. doi: 10.3389/fcvm.2022.960403



# Clinical evaluation of the Multimapping technique for simultaneous myocardial $T_1$ and $T_2$ mapping

Charlotta Jarkman[1], Carl-Johan Carlhäll[1,2,3†] and Markus Henningsson[1,2*†]

[1]Department of Clinical Physiology in Linköping, Department of Health, Medicine and Caring Sciences, Linköping University, Linköping, Sweden, [2]Division of Diagnostics and Specialist Medicine, Department of Health, Medicine and Caring Sciences (HMV), Linköping University, Linköping, Sweden, [3]Center for Medical Image Science and Visualization (CMIV), Linköping University, Linköping, Sweden

The Multimapping technique was recently proposed for simultaneous myocardial $T_1$ and $T_2$ mapping. In this study, we evaluate its correlation with clinical reference mapping techniques in patients with a range of cardiovascular diseases (CVDs) and compare image quality and inter- and intra-observer repeatability. Multimapping consists of an ECG-triggered, 2D single-shot bSSFP readout with inversion recovery and $T_2$ preparation modules, acquired across 10 cardiac cycles. The sequence was implemented at 1.5T and compared to clinical reference mapping techniques, modified Look-Locker inversion recovery (MOLLI) and $T_2$ prepared bSSFP with four echo times ($T_2$bSSFP), and compared in 47 patients with CVD (of which 44 were analyzed). In diseased myocardial segments (defined as the presence of late gadolinium enhancement), there was a high correlation between Multimapping and MOLLI for native myocardium $T_1$ ($r^2 = 0.73$), ECV ($r^2 = 0.91$), and blood $T_1$ ($r^2 = 0.88$), and Multimapping and $T_2$bSSFP for native myocardial $T_2$ ($r^2 = 0.80$). In healthy myocardial segments, a bias for native $T_1$ (Multimapping = 1,116 ± 21 ms, MOLLI = 1,002 ± 21, $P < 0.001$), post-contrast $T_1$ (Multimapping = 479 ± 31 ms, MOLLI = 426 ± 27 ms, 0.001), ECV (Multimapping = 21.5 ± 1.9%, MOLLI = 23.7 ± 2.3%, $P = 0.001$), and native $T_2$ (Multimapping = 48.0 ± 3.0 ms, $T_2$bSSFP = 53.9 ± 3.5 ms, $P < 0.001$) was observed. The image quality for Multimapping was scored as higher for all mapping techniques (native $T_1$, post-contrast $T_1$, ECV, and $T_2$bSSFP) compared to the clinical reference techniques. The inter- and intra-observer agreements were excellent (intraclass correlation coefficient, ICC > 0.9) for most measurements, except for inter-observer repeatability of Multimapping native $T_1$ (ICC = 0.87), post-contrast $T_1$ (ICC = 0.73), and $T_2$bSSFP native $T_2$ (ICC = 0.88). Multimapping shows high correlations with clinical reference mapping techniques for $T_1$, $T_2$, and ECV in a diverse cohort of patients with different cardiovascular diseases. Multimapping enables simultaneous $T_1$ and $T_2$ mapping and can be performed in a short breath-hold, with image quality superior to that of the clinical reference techniques.

KEYWORDS

**T1 mapping, T2 mapping, ECV, quantitative CMR, simultaneous multiparametric CMR**

# Introduction

Myocardial $T_1$ and/or $T_2$ values are altered in many cardiovascular diseases (1). $T_1$ and $T_2$ quantification, along with disease-specific patterns of regional and global distribution, can be captured with myocardial mapping techniques (2). In the last 15–20 years, a number of $T_1$ and $T_2$ mapping techniques have been published, with different strengths and weaknesses in terms of quantification accuracy, precision, scan time, spatial resolution, and coverage (3). Despite being one of the first $T_1$ mapping techniques, the modified Look-Locker inversion recovery (MOLLI) remains the most clinically used method due to its high precision and availability on all major scanner platforms (4, 5). However, MOLLI $T_1$ accuracy is relatively low, and the quantification is susceptible to confounding effects from heart rate or $T_2$-dependent variability, magnetization transfer effects, motion artifacts, and system imperfections (5, 6). Different $T_1$ mapping methods have been proposed to address these shortcomings, yet have failed to make significant inroads in the market share of clinical use (7–11). Myocardial $T_2$ mapping can be performed with multi-echo spin-echo or $T_2$-prepared balanced steady-state free precession ($T_2$bSSFP) techniques (12–14). The latter approach is likely the most widely used clinically due to its relative robustness to physiological motion.

In recent years, there has been a growing interest in techniques to simultaneously map $T_1$ and $T_2$ in a single scan (15–21). Advantages of this approach compared to conventional mapping, which is performed separately for $T_1$ and $T_2$, are that the images are intrinsically spatially aligned, scan time is typically shorter, and the confounding effects of $T_1$ or $T_2$ on the quantification of the opposite parameter are minimized. Despite the many theoretical advantages of simultaneous $T_1$ and $T_2$ mapping, there is a paucity of translational studies using these techniques in patients with cardiovascular disease (22, 23). This may be due to the more sophisticated acquisition, reconstruction, and mapping strategies necessary for such techniques, which pose challenges for clinical translation. Recently, a new technique for simultaneous $T_1$ and $T_2$ mapping, termed Multimapping, was proposed using a standard Cartesian trajectory and evaluated (primarily) in healthy subjects (24). Due to its simplicity, Multimapping may be readily applied in a clinical setting to enable the evaluation of simultaneous $T_1$ and $T_2$ mapping in patients with cardiovascular disease.

The primary aim of this study is to validate Multimapping $T_1$ and $T_2$ values against clinical reference techniques in patients with different cardiovascular diseases in terms of parameter quantification and image quality. The secondary aim of this study is to evaluate Multimapping intra- and inter-observer variability.

TABLE 1 Clinical characteristics.

| | |
|---|---|
| Patients (*n*) | 44 |
| Age (years) | 49 ± 20 |
| Male sex, *n* (%) | 28 (64) |
| BMI (kg/m2) | 25 ± 4 |
| Height (cm) | 176 ± 10 |
| Weight (kg) | 78 ± 12 |
| Heart rate (bpm) | 67 ± 14 |
| LVEF (%) | 53 ± 11 |
| LVSV (ml) | 94 ± 18 |
| LVEDV (ml) | 186 ± 54 |

BMI, body mass index; LVEF, left ventricular ejection fraction; LVSV, left ventricular stroke volume; LVEF, left ventricular end-diastolic volume.

# Materials and methods

## Study population

All patients provided written informed consent prior to participation, and the study was approved by the local ethics committee (Linköping Regional Ethics Committee, 2015/396–31) and conducted according to the Declaration of Helsinki. Patients referred for CMR at Linköping University Hospital between June and November 2021 were considered for inclusion in this study. In total, 47 patients were recruited. Datasets from three patients were excluded, two because no late gadolinium enhancement (LGE) images were acquired and one due to excessive fold-over artifacts. Clinical characteristics of the remaining patients can be seen in Table 1. Of the included patients, normal cardiac MRI scan was found in 15 (34.1%) patients, myocarditis in 11 (25%) patients, dilated cardiomyopathy (DCM) in 6 (13.6%) patients, ventricular hypertrophy (hypertrophic cardiomyopathy or hypertrophy of unknown origin) in 5 (11.4%) patients, ischemic myocardial injury (acute/recent or old) in 3 (6.8%) patients, arrhythmogenic right ventricular cardiomyopathy in 2 (4.5%) patients, pericarditis in 1 (2.3%) patient, and congenital heart disease in 1 (2.3%) patient.

## Data acquisition and reconstruction

All scans were performed on a 1.5T Philips clinical CMR scanner (Philips Healthcare, Best, The Netherlands) using a 28-channel torso coil. The Multimapping pulse sequence and post-processing steps are illustrated in Figure 1. Ten single-shot images are acquired across consecutive cardiac cycles using balanced steady-state free precession (bSSFP) readouts, triggered to the mid-diastolic rest period. Adiabatic inversion radiofrequency (RF) pulses with delay times of 300 ms are

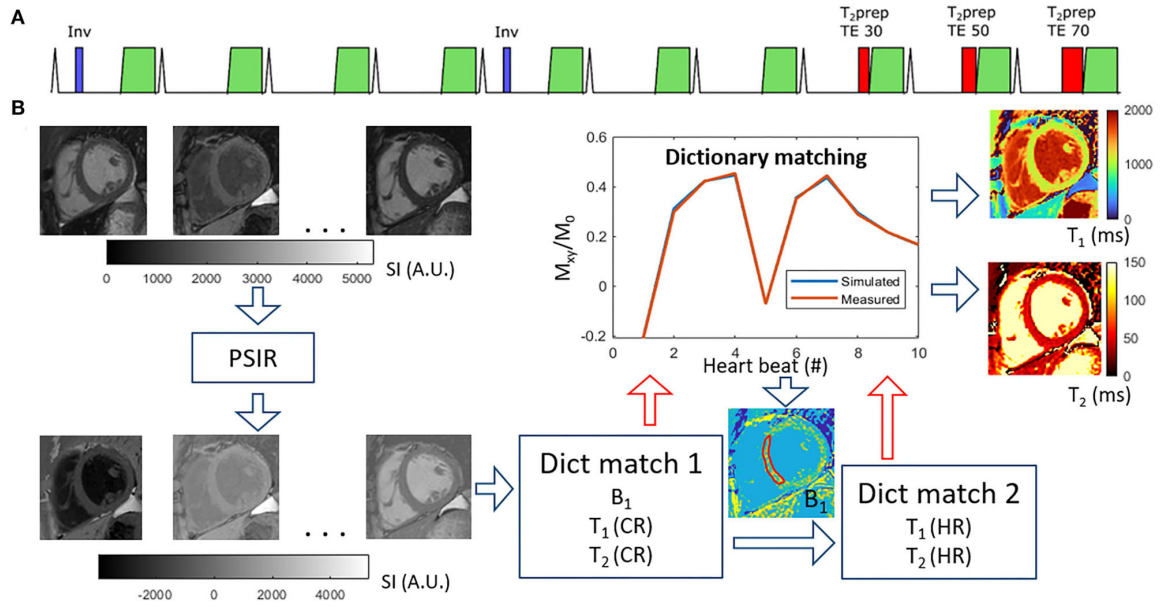


FIGURE 1
Multimapping pulse sequence **(A)** and post-processing **(B)**. The pulse sequence consists of ECG-triggered 2D single-shot acquisitions in 10 consecutive cardiac cycles, preceded by inversion pulses in cycles 1 and 5, and $T_2$prep with different echo times (TE) in cycles 8, 9, and 10. The post-processing involves first performing a phase-sensitive inversion recovery (PSIR) operation to restore the polarity of the signal, followed by an initial dictionary matching (Dict match 1) to estimate a global $B_1$ correction factor based on an ROI in the myocardial septum. The dictionary matching finds the pixel-wise closest match between acquired data and the simulated acquisition (with scan-specific delays) for different $T_1$, $T_2$, and RF scaling factor ($B_1$) combinations. A second dictionary matching step (Dict match 2) is then performed for only $T_1$ and $T_2$ with high temporal granularity (1 ms resolution) to generate the final $T_1$ and $T_2$ maps.

performed in the 1st and 5th cardiac cycles to improve $T_1$ sensitization. The inversion pulse used a hyperbolic secant shape, had a duration of 8.4 ms, and a $B_1$ amplitude of 13.5 μT. A previous study has shown that similar settings yield an inversion efficiency of approximately 0.89 (25), which was assumed for this study. $T_2$ preparation modules with hard 90° RF pulses and four adiabatic refocusing RF pulses are performed in the 8th, 9th, and 10th cardiac cycles to improve $T_2$ sensitization using echo times of 30, 50, and 70 ms, respectively. The Multimapping imaging parameters for all experiments are: field of view = 320×320 mm, spatial resolution = 2×2 mm, slice thickness = 10 mm, nominal flip angle = 50°, bandwidth = 1,076 Hz/pixel, TR = 2.3 ms, TE = 1.2 ms, SENSE factor = 2, linear profile order. Ten startup RF pulses are used with linearly increasing flip angles. The Multimapping scan was acquired in a mid-ventricular short-axis slice (except in one patient which was mistakenly acquired in a four-chamber view) during a breath-hold. Native Multimapping was acquired in all 47 patients, and post-contrast Multimapping was performed in 31 patients approximately 15 to 20 min after contrast agent administration (0.2 mmol/kg gadobutrol). Due to clinical prioritization, the post-contrast Multimapping was performed after the acquisition of post-contrast MOLL and LGE.

All Multimapping source images were reconstructed on the scanner and transferred to an offline workstation (Intel Core i7-8565U 1.80 GHz processor with 16Gb RAM) to generate $T_1$ and $T_2$ maps using MATLAB R2021b (The MathWorks, Natick, MA). The MATLAB code used to generate the maps, including example Multimapping source images from one subject, is available at https://github.com/Multimapping/Matlab_files. Since blood samples were not available for all patients, Multimapping synthetic ECV maps were generated using synthetic hematocrit values, based on the native MOLLI left ventricular blood pool measurements, as previously outlined (26). Image registration using a rigid body transformation was applied to spatially align the native and post-contrast $T_1$ maps prior to ECV calculation.

MOLLI was acquired in all 47 patients and $T_2$bSSFP was acquired in 45 patients, in the same slice as Multimapping and used as clinical reference techniques for $T_1$ and $T_2$ mapping, respectively. All imaging parameters for the reference techniques (field of view, spatial resolution, etc.) were the same as for Multimapping, except for the flip angle which was 35°. MOLLI was acquired with the 5 (3s) 3 scheme and used the same adiabatic inversion pulse as Multimapping. $T_2$bSSFP was acquired with four images at different $T_2$ preparation echo times (0, 23, 46, and 70 ms) and used 3 pause cardiac cycles between each image. Furthermore, $T_2$bSSFP used the same RF pulse types for the $T_2$ preparation module as Multimapping. The reference maps were reconstructed on the scanner using vendor-provided inline mapping algorithms, except for the ECV

maps which were generated offline using MATLAB. Similar to Multimapping, synthetic ECV maps were generated using a synthetic hematocrit value derived from the left ventricular blood pool $T_1$ measured in the native MOLLI image. As for Multimapping, image registration was applied to native and post-contrast MOLLI $T_1$ maps before ECV was calculated. LGE imaging parameters were TR/TE = 5.6/2.0 ms, flip angle = 25°, FOV = 350×350 $mm^2$, spatial resolution = 1.8×1.8 $mm^2$.

## Image analysis

$T_1$ (native and post-contrast), $T_2$ (native), and ECV measurements were made by drawing manual regions of interest (ROIs) in all datasets. To compare Multimapping to the clinical reference techniques, two sets of myocardial measurements were performed, one targeting any diseased myocardium and one targeting healthy myocardium. For the measurements of diseased myocardium in all maps, ROIs were drawn in the area corresponding with the most prominent positive LGE findings of each patient. Since only a subset of patients had positive LGE findings in the imaged slice, this resulted in 21 measurements for native $T_1$ and $T_2$ and 12 measurements for post-contrast $T_1$ and ECV. For the measurements of healthy myocardium in all maps, ROIs were drawn in the area remote of any LGE abnormality and preferentially in the interventricular septum if it was free of abnormal LGE. Patients were excluded from this analysis if there were indications suggestive of global or diffuse myocardial disease. The measurements in the healthy myocardium were performed in a total of 19 patients for native $T_1$, 12 patients for $T_1$ post-contrast and ECV, and 18 patients for $T_2$.

Measurements were performed in all patients by one observer (CJ, 1 year of CMR experience). To allow intra-observer variability analysis, measurements were repeated in 23 patients by the same observer 2 weeks later. For inter-observer variability analysis, the same 23 patients were measured by two additional observers (MH and CJC with 14 and 21 years of CMR experience, respectively). Furthermore, to compare blood $T_1$ (native and post-contrast), ROIs were drawn in the left ventricular blood pool (avoiding any papillary muscles) in the Multimapping $T_1$ and MOLLI images.

The image quality of the acquired maps was qualitatively compared using a Likert scale as devised by Jaubert et al. (22) with the following categories: 1 = uninterpretable, 2 = poor definition of edges, significant noise and/or residual artifacts, 3 = mildly blurred edges, mild noise and/or residual artifacts, 4 = slightly blurred edges, minor residual artifacts, and 5 = negligible blurring or residual artifacts. Visual scoring was performed for $T_1$ (native and post-contrast), $T_2$ (native), and ECV separately using the different mapping techniques, and this analysis was performed in 20 patients. The visual scoring was performed by consensus of two blinded observers (CJ and CJC).

## Statistical analysis

Continuous variables are expressed as mean ± SD. Categorical variables are expressed as counts and percentages. For the remote measurements, two-tailed Student's paired *t*-tests were performed to compare Multimapping to MOLLI for native $T_1$, post-contrast $T_1$, and ECV, and Multimapping and $T_2$bSSFP for native $T_2$. For the remote measurements, all parameters tested positive for normality using a Shapiro–Wilk test. Bland–Altman and correlation plots were used to evaluate the agreement and correlation, respectively, between Multimapping and the reference techniques of the measurements in diseased myocardium for native $T_1$, post-contrast $T_1$, ECV, and native $T_2$. To investigate any heart rate dependency for the mapping techniques, the measurements of the remote myocardium were correlated with the heart rate at the time of the scan. Similarly, dependency on $T_2$ for $T_1$ (and vice versa) was evaluated by correlating remote $T_1$ with $T_2$ for both Multimapping and the reference techniques, and testing for statistical significance. To account for multiple comparisons, Bonferroni correction was performed on the threshold for all significance tests. Since four comparisons were performed (native and post-contrast $T_1$, native $T_2$, and ECV), a threshold of 0.05/4 = 0.0125 was used. Intra-observer repeatability and inter-observer repeatability were assessed with intraclass correlation coefficient (ICC) analysis. ICC was calculated using absolute agreement two-way mixed model. Statistical analysis was performed using IBM SPSS Statistics, version 27.0.

# Results

Representative parameter maps acquired with Multimapping, reference techniques, and LGE in a patient with no cardiovascular disease findings are shown in Figure 2. Parameter maps from a patient with myocarditis are shown in Figure 3, with prominently altered quantitative values seen in both Multimapping and reference techniques. The final example, in Figure 4, shows parameter maps from a patient with myocardial infarction with a clearly delineated area of infarction in the Multimaps, correlating with LGE. Multimaps for all patients can be downloaded from https://github.com/Multimapping/Patient_study/raw/main/MapReconstructions.pdf.

## Comparison of Multimapping and reference techniques in remote myocardium

The Multimapping native $T_1$ was 1,116 ± 21 ms and for MOLLI 1,002 ± 21 ms, resulting in a statistically significant bias of 114 ms ($P < 0.001$). Multimapping post-contrast T1

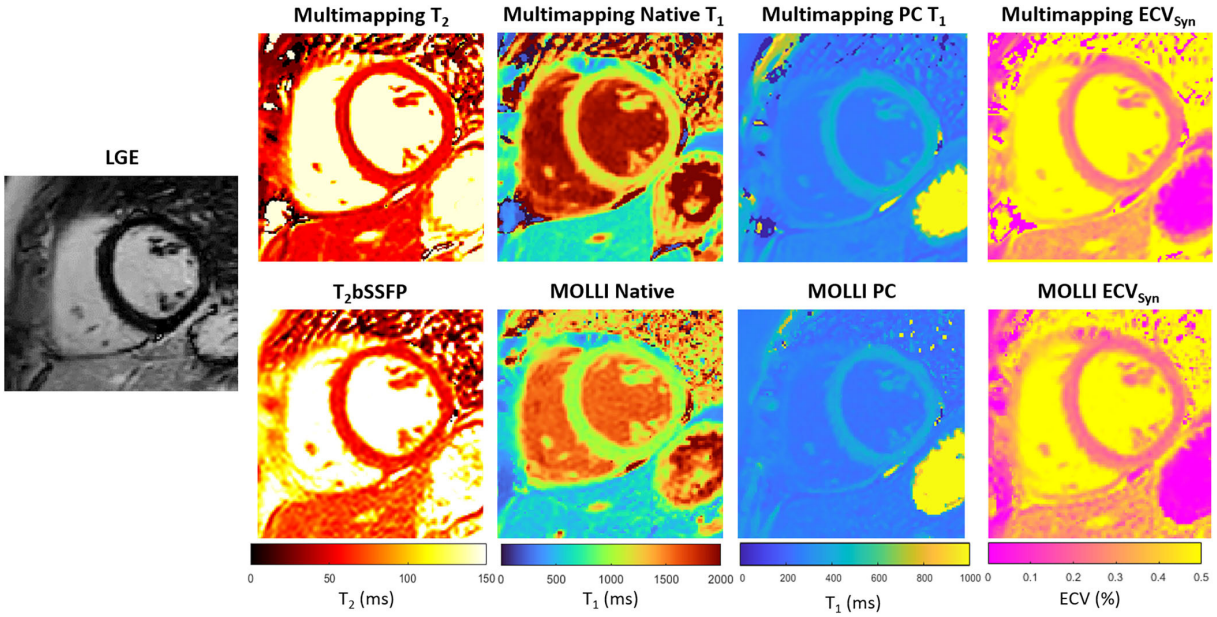


FIGURE 2
LGE and parameter maps (native $T_2$, native $T_1$, post-contrast $T_1$, and ECV) are shown for a patient with no cardiovascular disease findings. The parameter maps were acquired using either Multimapping (top row) or reference techniques (bottom row). Septal $T_2$ was 49.6 ms and 56.7 ms for Multimapping and $T_2$bSSFP, respectively. Septal (native/post-contrast) $T_1$ was 1,144/422 ms and 1,003/381 ms for Multimapping and MOLLI, respectively. Septal ECV was 24.9 and 23.8% for Multimapping and MOLLI, respectively.

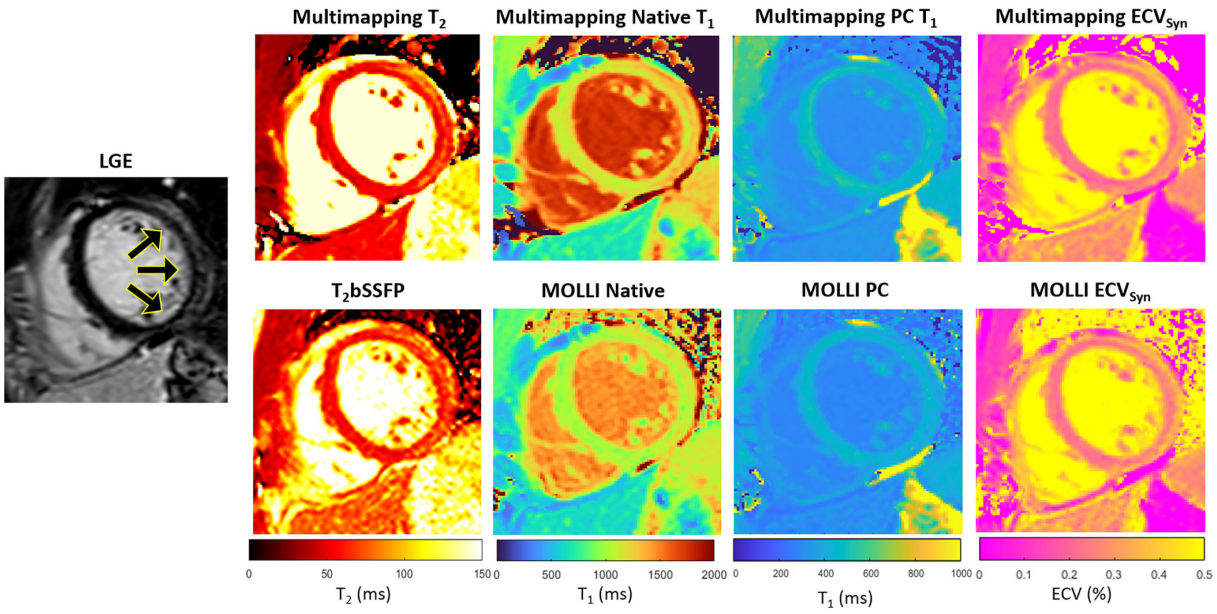


FIGURE 3
LGE and parameter maps in a patient with myocarditis, as indicated by the increased signal in the lateral wall in the LGE and also apparent as altered values in the parameter maps (Multimapping: top row, reference techniques: bottom row). Measurements in the area of enhancement (lateral wall) yielded $T_2$ of 65.7 ms and 62.4.6 ms for Multimapping and $T_2$bSSFP, respectively. $T_1$ values (native/post-contrast) in the same area were 1,286/446 ms and 1,111/423 ms for Multimapping and MOLLI, respectively. ECV was 26.6 and 28.3% in the enhanced area for Multimapping and MOLLI, respectively.

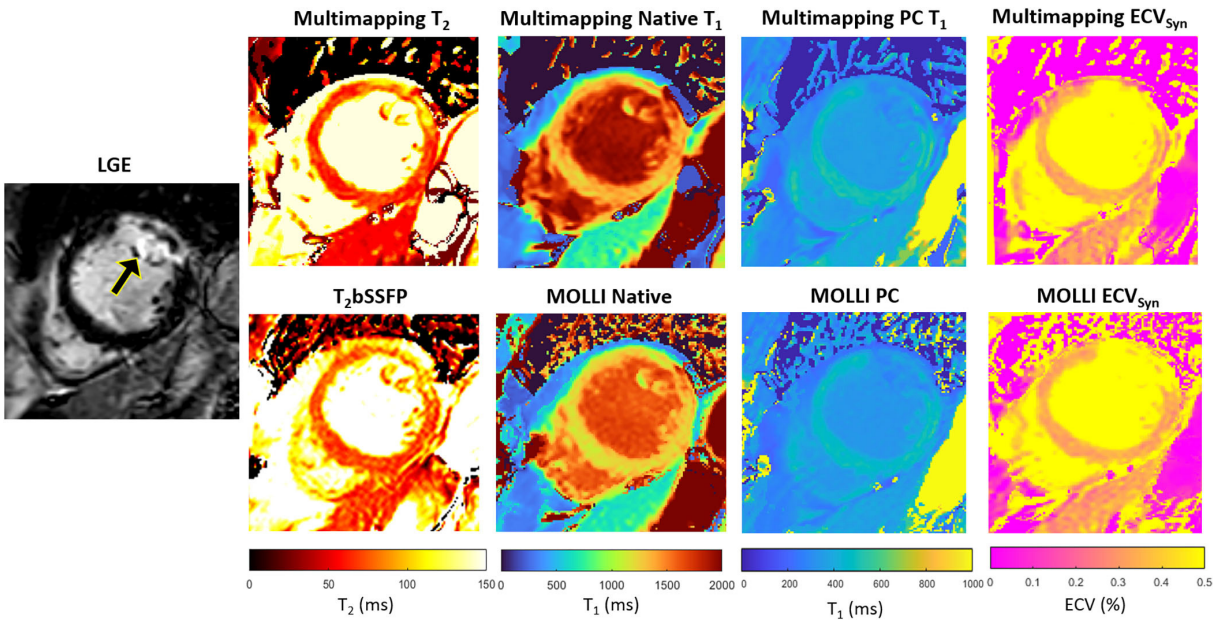


FIGURE 4
LGE and parameter maps in a patient with myocardial infarction, clearly visualized using all techniques, both native and post-contrast. Measurements in the area of enhancement (anterolateral segment) yielded $T_2$ of 90.5 ms and 88.6 ms for Multimapping and $T_2$bSSFP, respectively. $T_1$ values (native/post-contrast) in the same area were 1,516/355 ms and 1,440/338 ms for Multimapping and MOLLI, respectively. ECV was 33.3% and 33% in the enhanced area for Multimapping and MOLLI, respectively.

was 479 ± 31 ms and for MOLLI 426 ± 27 ms, yielding a bias of 53 ms which was statistically significant ($P < 0.001$). Multimapping ECV was 21.5 ± 1.9%, and MOLLI ECV was 23.7 ± 2.3%, resulting in a bias of −2.2% which was statistically significant ($P = 0.001$). Multimapping native $T_2$ was 48.0 ± 3.0 ms while $T_2$bSSFP was 53.9 ± 3.5 ms, a statistically significant bias of −9 ms ($P < 0.001$) (Figure 5).

There was no correlation between native $T_1$ and $T_2$ for neither Multimapping nor MOLLI and $T_2$bSSFP. Multimapping $T_1$ (native and post-contrast), $T_2$, or ECV and MOLLI $T_1$ (native and post-contrast) or ECV did not correlate with heart rate either. However, $T_2$bSSFP showed a correlation with heart rate ($P < 0.001$) (Figure 5).

## Comparison of Multimapping and reference techniques for diseased myocardium

In general, the correlation between Multimapping and the clinical reference techniques was very strong ($r^2 > 0.7$) for most variables (Figure 6). A strong correlation coefficient ($r^2 > 0.5$) was found between Multimapping and MOLLI for myocardial $T_1$ post-contrast ($r^2 = 0.66$) and blood $T_1$ post-contrast ($r^2 = 0.53$).

## Inter- and intra-observer variability

The myocardial measurements and measurements of the left ventricular blood pool for intra-repeatability assessment showed excellent repeatability (myocardial ICC > 0.97, LV blood pool ICC = 1.00) (Table 2). The myocardial measurements for inter-repeatability showed moderate to excellent repeatability (ICC > 0.73) for all mapping techniques. The native and post-contrast $T_1$ measurements of the blood pool for inter-repeatability showed good to excellent repeatability (ICC > 0.92).

## Image quality assessment

The image quality was scored significantly higher for Multimapping compared to $T_2$bSSFP ($P < 0.001$), MOLLI native $T_1$ ($P = 0.007$), MOLLI post-contrast $T_1$ ($P < 0.001$), and MOLLI ECV ($P < 0.001$) (Figure 7).

# Discussion

In this study, a new method for simultaneous $T_1$ and $T_2$ mapping was compared to the clinical reference mapping technique in a cohort of patients with cardiovascular disease. We found a strong to very strong correlation between the methods for all measured parameters (native $T_1$, post-contrast

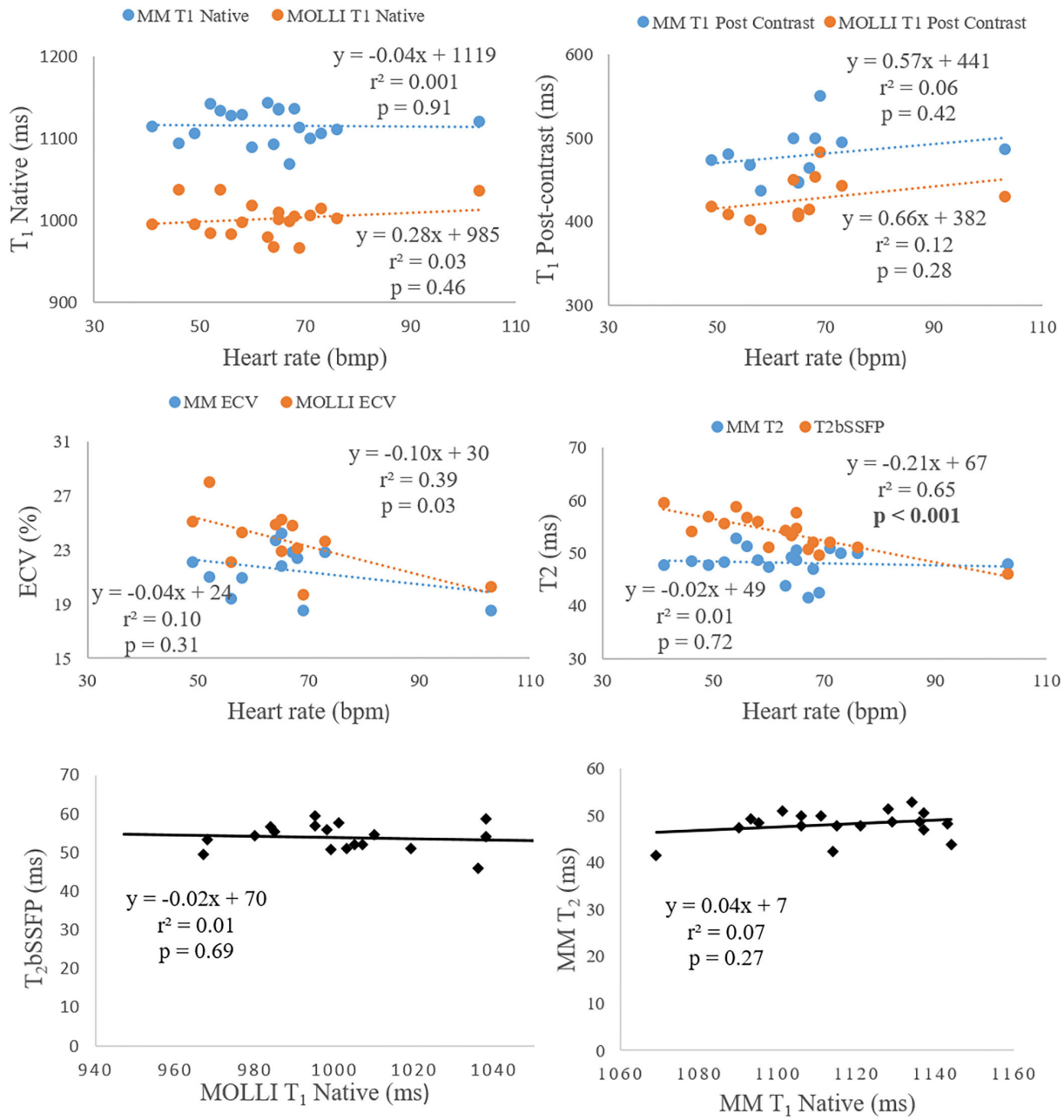


FIGURE 5
The two top rows show the correlation analysis of heart rate dependency to $T_1$ (native and post-contrast), ECV, and $T_2$. The bottom row shows the correlation analysis between native $T_1$ and $T_2$.

$T_1$, ECV, and native $T_2$), while the image quality was considered better using the proposed Multimapping technique compared to the reference methods. Furthermore, intra- and inter-observer variability of Multimapping parameter measurements were in general low and similar to those obtained with the clinical reference techniques.

In segments of healthy/remote myocardium, we measured a mean native $T_1$ of 1116 ms using Multimapping, more than 100 ms higher than for MOLLI. However, MOLLI is known to significantly underestimate $T_1$ when compared to more accurate methods such as SASHA (5), which typically yields native $T_1$ of around 1,200 ms at 1.5T (7, 27). The native $T_1$ Multimapping values are also in line with the previous study using this technique in healthy volunteers which measured 1,114 ms (24). For post-contrast $T_1$ mapping, there was also a significantly longer $T_1$ using Multimapping (479 ms) compared

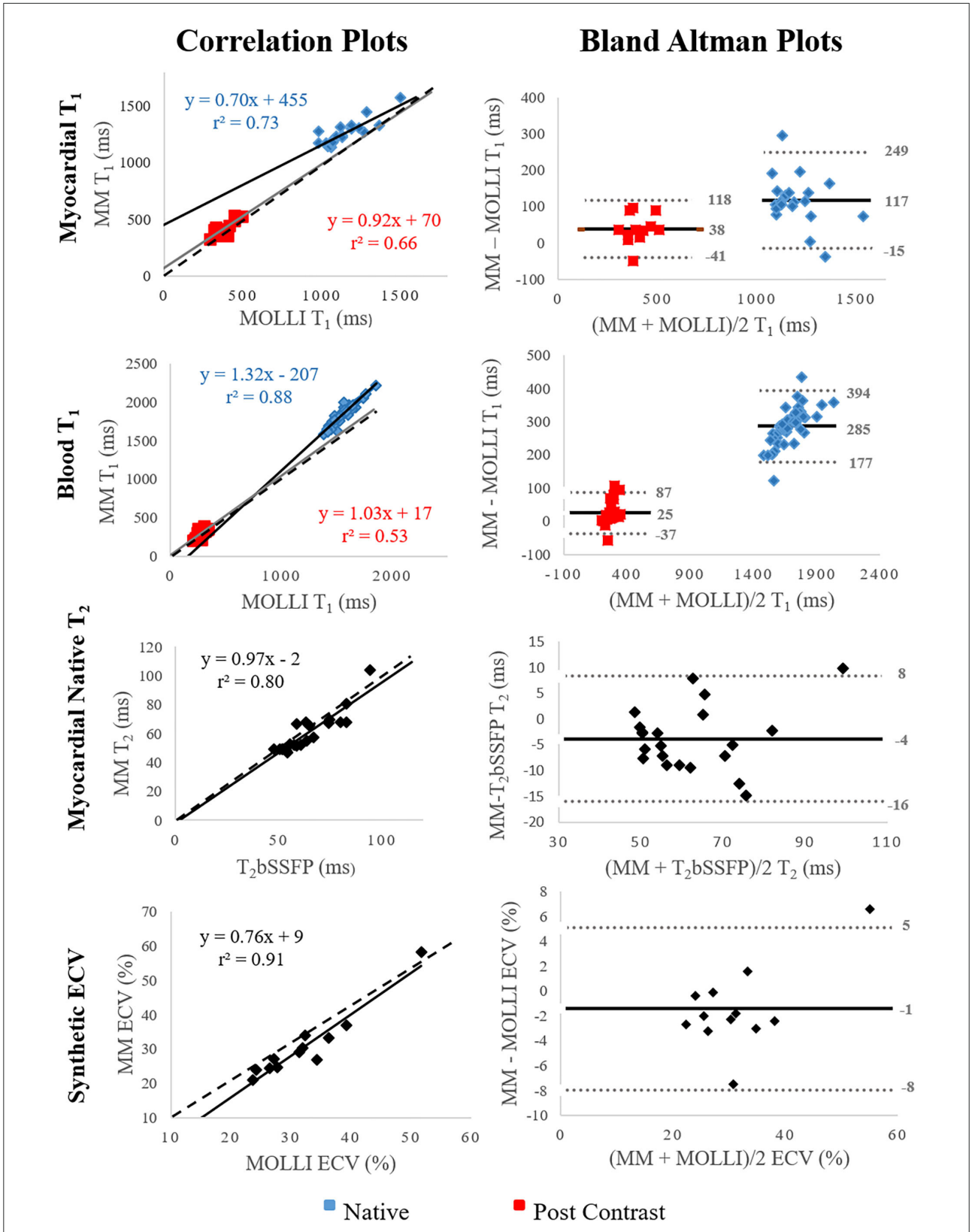


FIGURE 6
Correlation and Bland–Altman plots comparing Multimapping (MM) to MOLLI and $T_2$bSSFP. For the correlation plots, black and gray lines indicate line of best fit, and the dotted lines show the identity lines. The black lines indicate bias in the Bland–Altman plots. Correlation coefficient ($r^2$) is reported in the correlation plots and mean difference, and lower and upper limits of agreement (1.96 SD) in the Bland–Altman plots.

to MOLLI (427 ms). Although post-contrast $T_1$ values are more difficult to compare between studies due to differences in contrast agents and the timing of acquisition after injection, previous studies have shown underestimation of post-contrast $T_1$ for MOLLI compared to more accurate techniques such as SASHA (28, 29). The study by Nordlund et al. (29) also demonstrated that MOLLI overestimates ECV by approximately 4% in healthy volunteers compared to SASHA, the latter technique correlating more closely with radioisotopes in pigs. This suggests that the significantly lower ECV measured in this study with Multimapping (22%) may be more accurate compared to MOLLI (24%). However, the conversion from $T_1$ to hematocrit was based on the relationship established for MOLLI in a previous study, which may bias measurements if applied to Multimapping synthetic ECV. For Multimapping synthetic ECV to be used independently of MOLLI, then the relationship between Multimapping blood $T_1$ and hematocrit should be established. Alternatively, the hematocrit could be directly measured to calculate Multimapping ECV without the need for a MOLLI acquisition. Correlation of $T_1$ and $T_2$ values with potential confounding variables such as heart rate or the opposite ($T_2$ or $T_1$) parameter did not show any particular dependency for Multimapping in this regard. However, $T_2$bSSFP appeared to be inversely correlated with heart rate. This suggests additional delayed cardiac cycles may be required to yield less biased $T_2$ values for high heart rates. Conversely, Multimapping may be a more robust approach for $T_1$ and $T_2$ mapping at higher heart rates as no additional modification of the pulse sequence is required.

In the measurements of myocardial segments with disease, we found a high correlation between Multimapping and the clinical reference techniques for native $T_1$ (blood and myocardium), $T_2$, and ECV. While correlations for post-contrast $T_1$ (blood and myocardium) were more moderate, this may be explained by the confounding factor of time after injection, which affect the $T_1$ measurements. Furthermore, measured post-contrast $T_1$ in this study had a narrower range for both Multimapping and MOLLI compared to native $T_1$ which can contribute to a weaker correlation between techniques. Nevertheless, a very strong correlation between Multimapping and reference techniques for native $T_1$, $T_2$, and ECV indicates that Multimapping is a useful technique that can be used to detect disease.

Dictionary-based mapping techniques such as Multimapping typically assume that there is no through-plane motion, which is not the case for flowing blood. Such through-plane motion leads to $T_1$ overestimation as inflowing spins have seen fewer RF pulses and are therefore less saturated. This can explain the observed overestimation of blood (particularly native) $T_1$ relative to MOLLI. However, it should also be noted that, due to the strong correlation for native blood $T_1$ blood between Multimapping and MOLLI, the Multimapping technique can likely still capture variability in blood $T_1$ (due to, e.g., different hematocrit levels) with a similar sensitivity as MOLLI.

The image quality was superior using Multimapping compared to all clinical reference techniques. This could be due to the higher flip angle of 50° using Multimapping, compared to MOLLI and $T_2$bSSFP which both use a flip angle 35°, with otherwise identical imaging parameters to Multimapping. A higher flip angle for bSSFP-based mapping techniques leads to a higher signal-to-noise ratio which typically contributes to improved image quality. The shorter duration of Multimapping (10 beats) compared to both MOLLI (11 beats) and $T_2$bSSFP (16 beats) means that Multimapping is less prone to respiratory motion-induced misalignment, which may also contribute to a better image quality. While the Multimapping and MOLLI pulse sequences are very similar (both inversion recovery with bSSFP readouts), Multimapping benefits from phase-sensitive inversion recovery post-processing step which has been shown to improve $T_1$ map image quality compared to fitting with magnitude images (30), used in the vendor-provided fitting algorithm for MOLLI. Compared to Multimapping, $T_2$bSSFP uses significantly fewer source images for $T_2$ mapping, and while only three $T_2$ preparation modules are included in the Multimapping pulse sequence, the bSSFP readout is intrinsically $T_2/T_1$ weighted which contributes to the $T_2$ sensitivity and may explain the improved image quality.

The intra- and inter-observer repeatability analysis showed an excellent repeatability for most measurements using both Multimapping and reference techniques. While Multimapping post-contrast myocardial $T_1$ inter-observer ICC of 0.73 was relatively low compared to that of MOLLI (ICC = 0.95), post-contrast $T_1$ mapping is primarily used to generate ECV maps, and here, Multimapping and MOLLI yielded near identical ICC values of 0.94 and 0.93, respectively.

## Comparison with other simultaneous $T_1$ and $T_2$ mapping techniques

Several simultaneous $T_1$ and $T_2$ mapping techniques have been proposed over the last years, comparable to Multimapping. Published studies using similar methods in healthy volunteers are summarized in Table 3, including Multimapping (24). Multimapping has a shorter scan duration than nearly all other simultaneous $T_1$ and $T_2$ mapping techniques, requiring 10 beats, which is also shorter than both MOLLI and $T_2$bSSFP. As many patients with cardiovascular diseases struggle to hold their breath for an extended period, reducing the scan time of mapping techniques is important and has been the focus of several studies (11, 38). This is also in line with the endeavor of utilizing less time-consuming CMR protocols in order to improve the adoption of CMR in routine cardiovascular practice. Inversion recovery magnetization preparation pulses

TABLE 2 Inter- and intra-observer ICC (95% confidence interval).

| | Myocardium | | Blood pool | |
|---|---|---|---|---|
| | Intra-repeatability | Inter-repeatability | Intra-repeatability | Inter-repeatability |
| MM $T_1$ native | 0.99 (0.97–1.00) | 0.87 (0.76–0.94) | 1.00 (1.00–1.00) | 0.92 (0.85–0.96) |
| MOLLI $T_1$ native | 0.99 (0.97–0.99) | 0.93 (0.88–0.97) | 1.00 (1.00–1.00) | 0.97 (1.00–1.00) |
| MM $T_1$ PC | 0.99 (0.98–1.00) | 0.73 (0.54–0.86) | 1.00 (1.00–1.00) | 1.00 (1.00–1.00) |
| MOLLI $T_1$ PC | 0.97 (0.93–0.99) | 0.95 (0.90–0.98) | 1.00 (1.00–1.00) | 1.00 (1.00–1.00) |
| MM ECV | 0.99 (0.98–1.00) | 0.94 (0.89–0.97) | | |
| MOLLI ECV | 0.99 (0.97–0.99) | 0.93 (0.87–0.97) | | |
| MM $T_2$ | 0.99 (0.96–0.99) | 0.91 (0.82–0.95) | | |
| $T_2$bSSFP | 0.98 (0.94–0.99) | 0.88 (0.78–0.95) | | |

MM, Multimapping; ECV, extracellular volume fraction; MOLLI, modified Look-Locker inversion recovery; $T_2$bSSFP, $T_2$-prepared balanced steady-state free precession.

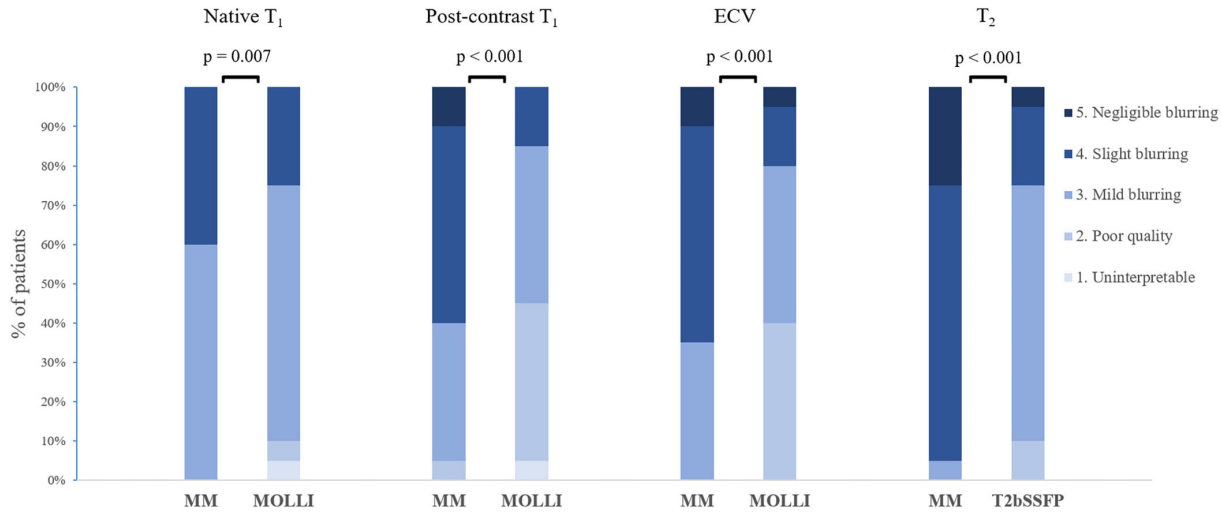


FIGURE 7
Distribution of image quality scores for Multimapping (MM) and *in vivo* reference techniques.

are often used for myocardial $T_1$ mapping as they increase quantification precision compared to saturation recovery (5), using the full dynamic range of the longitudinal magnetization, at the expense of accuracy as inversion pulses are more sensitive to confounding elements such as magnetization transfer and transverse relaxation during the pulses, which reduce their efficiency (6, 25, 39). Therefore, saturation recovery technique measurements are generally considered to be closer to the "true" *in vivo* $T_1$ times, typically several 100 ms higher than MOLLI on either 1.5T and 3T scanners. In this regard, Multimapping, which uses inversion recovery, generates $T_1$ values in healthy/remote myocardium of 1,116 ms, which is closer to the saturation recovery-based techniques (of approximately 1,200 ms) than MOLLI (approximately 1,000 ms) or the most comparable simultaneous $T_1$ and $T_2$ mapping studies, Blume et al. (15) and Jaubert et al. (33), which report a myocardial $T_1$ of 1,017 ms and 1,045 ms, respectively. This may be due to the assumed lower inversion efficiency of 0.89 for the inversion pulses, incorporated into the Multimapping signal model, which is likely closer to the true inversion efficiency than assuming perfect efficiency. However, the inversion efficiency potentially varies between field strengths and vendors, or even spatially across an image due to $B_0$ and $B_1$ inhomogeneity. Furthermore, the current Multimapping technique does not consider magnetization transfer. To yield more accurate $T_1$ values, reproducible across scanner platforms, these confounding effects should be included in the Multimapping signal model, preferably on a pixel-wise basis, although this will likely negatively impact the precision.

It can be difficult to precisely pinpoint the sources of differences in $T_1$ and $T_2$ values for the different techniques outlined in Table 3, particularly as many techniques rely on the unconventional acquisition, reconstruction, and mapping strategies. These include, for example, non-Cartesian

TABLE 3 Comparable published simultaneous $T_1$ and $T_2$ mapping techniques.

| Study | Scan time | FB/BH | IR/SR | Readout | Subjects | Additional mapping | Field strength | Native T1 (ms) | Native T2 (ms) |
|---|---|---|---|---|---|---|---|---|---|
| Blume et al. (15) | Around 3 min | FB | IR | 2D cartesian bSSFP | 19 HV | - | 1.5T | 1,017 ± 91 | 50 ± 4 |
| Kvernby et al. (17) | 15 beats | BH | IR | 3D Cartesian GRE | 10 HV | - | 3T | 1,083 ± 43 | 50.4 ± 3.6 |
| Akçakaya et al. (18) | 13 beats | BH | SR | 2D cartesian bSSFP | 10 HV | - | 1.5T | 1,210 ± 24 | 48.2 ± 2.8 |
| Santini et al. (31) | 8 beats | BH | IR | 2D cartesian bSSFP | 5 HV | - | 3T | 1,227 ± 68 | 37.9 ± 2.4 |
| Hamilton et al. (32) | 15 beats | BH | IR | 2D spiral GRE | 11 HV | - | 3T | 1,235, range 1,199 −1,316 | 38, range 32–43 |
| Jaubert et al. (33) | 15 beats | BH | IR | 2D radial ME-GRE | 10 HV | PDFF | 1.5T | 1,045 ± 32 | 42.8 ± 2.6 |
| Christodoulou et al. (19) | 88 s | FB | IR | 2D radial GRE | 10 HV | Cardiac motion | 3T | 1,216 ± 67 | 47.8 ± 4.9 |
| Shao et al. (34) | 11 beats | BH | IR | 2D radial GRE | 10 HV | - | 3T | 1,366 ± 31 | 37.4 ± 0.9 |
| Guo et al. (35) | 1.4 ± 0.3 min (WH) | FB | SR | M2D Cartesian bSSFP | 13 HV | - | 3T | 1,373 ± 50 | 48.7 ± 2.5 |
| Hermann et al. (36) | 18.5 s (+resp gating) | FB | SR | 2D cartesian ME-GRE | 10 HV | T2* | 3T | 1,573 ± 86 | 33.2 ± 3.6 |
| Chow et al. (37) | 11 beats | BH | SR | 2D cartesian bSSFP | 10 HV | - | 3T | 1,523 ± 18 | 36.7 ± 1.1 |
| Jarkman et al. | 10 beats | BH | IR | 2D cartesian bSSFP | Remote myocardium 19 patients | - | 1.5T | 1,116 ± 21 | 48.0 ± 3.0 |

WH, whole heart; FB, free breathing; BH, breath-hold; IR, inversion recovery; SR, saturation recovery; bSSFP, balanced steady-state free precession; GRE, spoiled gradient echo; ME-GRE, multi-echo spoiled gradient echo; M2D, multi-slice 2D; HV, healthy volunteer; PDFF, proton density fat fraction.

(radial or spiral) trajectories with iterative reconstruction algorithm, coupled with sophisticated and advanced mapping techniques which may be difficult to reproduce. In contrast, the Multimapping pulse sequence consists of a MOLLI-like acquisition scheme (inversion recovery with Cartesian single-shot 2D bSSFP readout) which are available on all major vendor platforms, with the addition of $T_2$prep modules which have also been implemented on all vendor platforms. For transparency, the Multimapping parameter mapping method using dictionary matching has been provided open source to enable reproduction of this technique by other investigators which may also enable direct comparison of Multimapping with other simultaneous $T_1$ and $T_2$ mapping techniques.

## Limitations

This study has several limitations: no respiratory motion correction was performed. Correcting for respiratory-induced image misalignment is important even for breath-held scans and can be achieved using image registration (40). Although image registration could be readily applied to Multimapping source image to this end, this was not performed in order to have a fair comparison with MOLLI and $T_2$bSSFP maps which were generated using inline vendor algorithm without motion correction. A second technical limitation of Multimapping is that manual interaction is required to define an ROI in the myocardial septum for the $B_1$ estimation. However, this is a relatively simple step, comparable to the input required to define ROIs for ECV maps. Further work is required to automatize this step or to incorporate $B_1$ in the high-resolution $T_1$ and $T_2$ dictionary matching, which would obviate the need for any manual interaction but with a potential penalty to the precision. A study limitation is that the patient cohort consisted of a small, heterogeneous population of patients with various cardiovascular diseases and performed on a single 1.5T Philips scanner. Further studies are required to evaluate the performance of Multimapping at 3T and using

other vendors. The evaluation of heart rate dependence of the mapping techniques was limited by the relatively narrow heart rates of nearly all patients (only one with heart rate over 100 bpm).

## Conclusions

Multimapping $T_1$ and $T_2$ values show high correlations with clinical reference mapping techniques in a diverse cohort of patients with different cardiovascular diseases. Multimapping enables simultaneous $T_1$ and $T_2$ mapping and can be performed in a short (10 cardiac beats) breath-hold, with image quality superior to that of the clinical reference techniques.

## Data availability statement

The dataset presented in this study can be found in online at: https://github.com/Multimapping/Patient_study/raw/main/MapReconstructions.pdf.

## Ethics statement

The studies involving human participants were reviewed and approved by Linköping Regional Ethics Committee. The patients/participants provided their written informed consent to participate in this study. Written informed consent was obtained from the individual(s) for the publication of any potentially identifiable images or data included in this article.

## Author contributions

MH and C-JC conceived of the study. MH developed the methods, acquired the data, and performed image reconstruction and processing. MH, CJ, and C-JC analyzed the data. All authors participated in revising the manuscript, read, and approved the final manuscript.

## Funding

The research leading to these results has received funding from the Swedish Medical Research Council [2018-02779], the Swedish Heart and Lung Foundation [20170440], ALF Grants Region Östergötland [LIO-797721], and the Swedish Research Council [2018-04164].

## Conflict of interest

The authors declare that the research was conducted in the absence of any commercial or financial relationships that could be construed as a potential conflict of interest.

## Publisher's note

All claims expressed in this article are solely those of the authors and do not necessarily represent those of their affiliated organizations, or those of the publisher, the editors and the reviewers. Any product that may be evaluated in this article, or claim that may be made by its manufacturer, is not guaranteed or endorsed by the publisher.

## References

1. Messroghli DR, Moon JC, Ferreira VM, Grosse-Wortmann L, He T, Kellman P, et al. Clinical recommendations for cardiovascular magnetic resonance mapping of T1, T2, T2 and extracellular volume: a consensus statement by the Society for Cardiovascular Magnetic Resonance (SCMR) endorsed by the European association for cardiovascular imagin. *J Cardiovasc Magn Reson.* (2017) 19:75. doi: 10.1186/s12968-017-0389-8

2. Kim PK, Hong YJ, Im DJ, Suh YJ, Park CH, Kim JY, et al. Myocardial T1 and T2 mapping: techniques and clinical applications. *Korean J Radiol.* (2017) 18:113–31. doi: 10.3348/kjr.2017.18.1.113

3. Ogier AC, Bustin A, Cochet H, Schwitter J, van Heeswijk RB. The road toward reproducibility of parametric mapping of the heart: a technical review. *Front Cardiovasc Med.* (2022) 9:876475. doi: 10.3389/fcvm.2022.876475

4. Messroghli DR, Radjenovic A, Kozerke S, Higgins DM, Sivananthan MU, Ridgway JP. Modified look-locker inversion recovery (MOLLI) for high-resolution T1 mapping of the heart. *Magn Reson Med.* (2004) 52:141–6. doi: 10.1002/mrm.20110

5. Kellman P, Hansen MS. T1-mapping in the heart: accuracy and precision. *J Cardiovasc Magn Reson.* (2014) 16:2. doi: 10.1186/1532-429X-16-2

6. Robson MD, Piechnik SK, Tunnicliffe EM, Neubauer S. T1 measurements in the human myocardium: The effects of magnetization transfer on the SASHA and MOLLI sequences. *Magn Reson Med.* (2013) 70:664–70. doi: 10.1002/mrm.24867

7. Chow K, Flewitt JA, Green JD, Pagano JJ, Friedrich MG, Thompson RB. Saturation recovery single-shot acquisition (SASHA) for myocardial T1 mapping. *Magn Reson Med.* (2014) 71:2082–95. doi: 10.1002/mrm.24878

8. Weingärtner S, Akçakaya M, Basha T, Kissinger K V, Goddu B, Berg S, et al. Combined saturation/inversion recovery sequences for improved evaluation of scar and diffuse fibrosis in patients with arrhythmia or heart rate variability. *Magn Reson Med.* (2014) 71:1024–34. doi: 10.1002/mrm.24761

9. Weingärtner S, Roujol S, Akçakaya M, Basha TA, Nezafat R. Free-breathing multislice native myocardial T1 mapping using the slice-interleaved T1 (STONE) sequence. *Magn Reson Med.* (2015) 74:115–24. doi: 10.1002/mrm.25387

10. Marty B, Coppa B, Carlier PG. Fast, precise, and accurate myocardial T1 mapping using a radial MOLLI sequence with FLASH readout. *Magn Reson Med.* (2018) 79:1387–98. doi: 10.1002/mrm.26795

11. Piechnik SK, Ferreira VM, Dall'Armellina E, Cochlin LE, Greiser A, Neubauer S, et al. Shortened Modified Look-Locker Inversion recovery (ShMOLLI) for clinical myocardial T1-mapping at 1.5 and 3 T within a 9 heartbeat breathhold. *J Cardiovasc Magn Reson.* (2010) 12:69. doi: 10.1186/1532-429X-12-69

12. Baeßler B, Schaarschmidt F, Stehning C, Schnackenburg B, Maintz D, Bunck AC. Cardiac T2-mapping using a fast gradient echo spin echo sequence - First *in vitro* and *in vivo* experience. *J Cardiovasc Magn Reson.* (2015) 17:67. doi: 10.1186/s12968-015-0177-2

13. Ding H, Fernandez-De-Manuel L, Schär M, Schuleri KH, Halperin H, He L, et al. Three-dimensional whole-heart T2 mapping at 3T. *Magn Reson Med.* (2015) 74:803–16. doi: 10.1002/mrm.25458

14. Sprinkart AM, Luetkens JA, Träber F, Doerner J, Gieseke J, Schnackenburg B, et al. Gradient Spin Echo (GraSE) imaging for fast myocardial T2 mapping. *J Cardiovasc Magn Reson.* (2015) 17:12. doi: 10.1186/s12968-015-0127-z

15. Blume U, Lockie T, Stehning C, Sinclair S, Uribe S, Razavi R, et al. Interleaved T1 and T2 relaxation time mapping for cardiac applications. *J Magn Reson Imaging.* (2009) 29:480–7. doi: 10.1002/jmri.21652

16. Shao J, Zhou Z, Nguyen KL, Finn JP, Hu P. Accurate, precise, simultaneous myocardial T1 and T2 mapping using a radial sequence with inversion recovery and T2 preparation. *NMR Biomed.* (2019) 32:e4165. doi: 10.1002/nbm.4165

17. Kvernby S, Warntjes MJ a. B, Haraldsson H, Carlhäll CJ, Engvall J, Ebbers T. Simultaneous three-dimensional myocardial T1 and T2 mapping in one breath hold with 3D-QALAS. *J Cardiovasc Magn Reson.* (2014) 16:102. doi: 10.1186/s12968-014-0102-0

18. Akçakaya M, Weingärtner S, Basha TA, Roujol S, Bellm S, Nezafat R. Joint myocardial T1 and T2 mapping using a combination of saturation recovery and T2-preparation. *Magn Reson Med.* (2016) 76:888–96. doi: 10.1002/mrm.25975

19. Christodoulou AG, Shaw JL, Nguyen C, Yang Q, Xie Y, Wang N, et al. Magnetic resonance multitasking for motion-resolved quantitative cardiovascular imaging. *Nat Biomed Eng.* (2018) 2:215–26. doi: 10.1038/s41551-018-0217-y

20. Milotta G, Bustin A, Jaubert O, Neji R, Prieto C, Botnar RM. 3D whole-heart isotropic-resolution motion-compensated joint T1/T2 mapping and water/fat imaging. *Magn Reson Med.* (2020) 84:3009–26. doi: 10.1002/mrm.28330

21. Mao X, Lee H-L, Hu Z, Cao T, Han F, Ma S, et al. Simultaneous multi-slice cardiac MR multitasking for motion-resolved, non-ECG, free-breathing T1–T2 mapping. *Front Cardiovasc Med.* (2022) 9:833257. doi: 10.3389/fcvm.2022.833257

22. Jaubert O, Cruz G, Bustin A, Hajhosseiny R, Nazir S, Schneider T, et al. T1, T2, and fat fraction cardiac MR fingerprinting: preliminary clinical evaluation. *J Magn Reson Imaging.* (2021) 53:1253–65. doi: 10.1002/jmri.27415

23. Cavallo AU, Liu Y, Patterson A, Al-Kindi S, Hamilton J, Gilkeson R, et al. CMR Fingerprinting for Myocardial T1, T2, and ECV quantification in patients with nonischemic cardiomyopathy. *JACC Cardiovasc Imaging.* (2019) 12:1584–5. doi: 10.1016/j.jcmg.2019.01.034

24. Henningsson M. Cartesian dictionary-based native T1 and T2 mapping of the myocardium. *Magn Reson Med.* (2022) 87:2347–62. doi: 10.1002/mrm.29143

25. Kellman P, Herzka DA, Hansen MS. Adiabatic inversion pulses for myocardial T1 mapping. *Magn Reson Med.* (2014) 71:1428–34. doi: 10.1002/mrm.24793

26. Fent GJ, Garg P, Foley JRJ, Swoboda PP, Dobson LE, Erhayiem B, et al. Synthetic Myocardial Extracellular Volume Fraction. *JACC Cardiovasc Imaging.* (2017) 10:1402–4. doi: 10.1016/j.jcmg.2016.12.007

27. Roujol S, Weingärtner S, Foppa M, Chow K, Kawaji K, Ngo LH, et al. Accuracy, precision, and reproducibility of four T1 mapping sequences: a head-to-head comparison of MOLLI, ShMOLLI, SASHA, and SAPPHIRE. *Radiology.* (2014) 272:683–9. doi: 10.1148/radiol.14140296

28. Weingärtner S, Meßner NM, Budjan J, Loßnitzer D, Mattler U, Papavassiliu T, et al. Myocardial T1-mapping at 3T using saturation-recovery: reference values, precision and comparison with MOLLI. *J Cardiovasc Magn Reson.* (2016) 18:84. doi: 10.1186/s12968-016-0302-x

29. Nordlund D, Xanthis C, Bidhult S, Jablonowski R, Kanski M, Kopic S, et al. Measuring extracellular volume fraction by MRI: first verification of values given by clinical sequences. *Magn Reson Med.* (2020) 83:662–72. doi: 10.1002/mrm.27938

30. Xue H, Greiser A, Zuehlsdorff S, Jolly MP, Guehring J, Arai AE, et al. Phase-sensitive inversion recovery for myocardial T1 mapping with motion correction and parametric fitting. *Magn Reson Med.* (2013) 69:1408–20. doi: 10.1002/mrm.24385

31. Santini F, Kawel-Boehm N, Greiser A, Bremerich J, Bieri O. Simultaneous T1 and T2 quantification of the myocardium using Cardiac Balanced-SSFP Inversion Recovery with Interleaved Sampling Acquisition (CABIRIA). *Magn Reson Med.* (2015) 74:365–71. doi: 10.1002/mrm.25402

32. Hamilton JI, Jiang Y, Chen Y, Ma D, Lo WC, Griswold M, et al. MR fingerprinting for rapid quantification of myocardial T1, T2, and proton spin density. *Magn Reson Med.* (2017) 77:1446–58. doi: 10.1002/mrm.26216

33. Jaubert O, Cruz G, Bustin A, Schneider T, Lavin B, Koken P, et al. Water–fat Dixon cardiac magnetic resonance fingerprinting. *Magn Reson Med.* (2020) 83:2107–23. doi: 10.1002/mrm.28070

34. Shao J, Ghodrati V, Nguyen KL, Hu P. Fast and accurate calculation of myocardial T1 and T2 values using deep learning Bloch equation simulations (DeepBLESS). *Magn Reson Med.* (2020) 84:2831–45. doi: 10.1002/mrm.28321

35. Guo R, Cai X, Kucukseymen S, Rodriguez J, Paskavitz A, Pierce P, et al. Free-breathing simultaneous myocardial T1 and T2 mapping with whole left ventricle coverage. *Magn Reson Med.* (2021) 85:1308–21. doi: 10.1002/mrm.28506

36. Hermann I, Kellman P, Demirel OB, Akçakaya M, Schad LR, Weingärtner S. Free-breathing simultaneous T1, T2, and T2∗ quantification in the myocardium. *Magn Reson Med.* (2021) 86:1226–40. doi: 10.1002/mrm.28753

37. Chow K, Hayes G, Flewitt JA, Feuchter P, Lydell C, Howarth A, et al. Improved accuracy and precision with three-parameter simultaneous myocardial T1 and T2 mapping using multiparametric SASHA. *Magn Reson Med.* (2022) 87:2775–91. doi: 10.1002/mrm.29170

38. Guo R, El-Rewaidy H, Assana S, Cai X, Amyar A, Chow K, et al. Accelerated cardiac T1 mapping in four heartbeats with inline MyoMapNet: a deep learning-based T1 estimation approach. *J Cardiovasc Magn Reson.* (2022) 24:6. doi: 10.1186/s12968-021-00834-0

39. Chow K, Kellman P, Spottiswoode BS, Nielles-Vallespin S, Arai AE, Salerno M, et al. Saturation pulse design for quantitative myocardial T1 mapping. *J Cardiovasc Magn Reson.* (2015) 17:84. doi: 10.1186/s12968-015-0187-0

40. Roujol S, Foppa M, Weingärtner S, Manning WJ, Nezafat R. Adaptive registration of varying contrast-weighted images for improved tissue characterization (ARCTIC): application to T1 mapping. *Magn Reson Med.* (2015) 73:1469–82. doi: 10.1002/mrm.25270